**Supplemental Methods**

*Generation of hCD19 CAR transgenic mice*

The anti-human CD19 antibody FMC63[1] scFv sequence was cloned in frame to the mouse CD8α transmembrane and mouse 4-1BB and CD3ζ intracellular domain sequences with 5' EcoRI and 3' XbaI sites. This fragment was subcloned into the phCD2 vector, which confers T cell-specific expression.[2] The plasmid sequence was removed by KpnI and NotI cleavage and gel-purified insert DNA was injected into C57BL/6 embryos and randomly integrated into the mouse genome. CAR transgenic (CAR-Tg) mice were bred on a C57BL/6 background and crossed to Thy1.1 and Rosa26-Cas9 knock-in mice. Progeny were analyzed for CAR expression by PCR analysis of genomic DNA and flow cytometric analysis of blood.

*In vitro cytotoxicity assays*

Spleens and peripheral lymph nodes from CAR-Tg or B6 control mice were harvested, processed into a single cell suspension, and treated with ACK buffer (Quality Biological 118-156-101) for red blood cell lysis. Cells were resuspended at 1–2x$10^6$ cells/ml in complete Click's medium (Thermo Fisher NC0118954) plus 25 U/ml recombinant hIL-2 and 2 μg/ml anti-mouse CD28 and cultured for 2-3 days on 6 well plates pre-coated with 2 μg/ml anti-mouse CD3. Cells were transferred to fresh plates and passaged with IL-2-suplemented medium. Six days after initial activation, cultures containing activated CAR-T or control T cells were cultured with 1x$10^5$ $hCD19^-$ or $hCD19^+$ B-ALL cells at the indicated ratios in complete Click's media without IL-2 for 24-48 hours. Samples were analyzed by quantitative flow cytometry with TruCount beads (BD Biosciences) to assess

the number of surviving B-ALL cells. Percent live tumor cells (% of control) = (# live target cells in sample/ # live target cells in control wells) x 100%.

*In vivo survival analysis*

C57BL/6 mice received $1\times10^6$ luciferase-expressing hCD19$^+$ B-ALL cells by i.v. tail vein injection, followed 6 days later by treatment with PBS (Gibco), control or CAR-T cells administered retro-orbitally. In experiments with CD8$^+$ cells only, $5x10^6$ MACS-purified activated CD8$^+$ T cells were injected. In experiments with both CD4$^+$ and CD8$^+$ cells, $5\times10^6$ CD4$^+$ and $5\times10^6$ CD8$^+$ MACS-purified activated T cells were administered together ($1x10^7$ total cells). For secondary tumor challenge, surviving mice received $5\times10^6$ hCD19$^+$ B-ALL cells by i.v. tail vein injection 50 days after initial CAR-T cell treatment. Tumor growth was monitored by bioluminescence imaging (Xenogen imaging system, Caliper Life Science).

*In vivo CAR-T cell co-transfers*

For WT and KO CAR co-transfers, activated CD8$^+$ cells were transduced with control non-targeting sgRNA (mCherry) or Regnase-1-targeting sgRNA (Ametrine) vectors to generate WT (mCherry$^+$Thy1.1$^+$Thy1.2$^+$) and KO CAR (Ametrine$^+$Thy1.1$^-$Thy1.2$^+$). Transduced cells were mixed 1:1 ($2.5\times10^6$ each; $5x10^6$ total cells) and administered to mice that had 6 days prior received hCD19$^+$ B-ALL cells or no tumor. For 4-way co-transfer, CD8$^+$ WT CAR-T (mCherry$^+$Thy1.1$^+$Thy1.2$^-$), KO CAR-T (Ametrine$^+$Thy1.1$^+$Thy1.2$^-$), WT B6 (mCherry$^+$Thy1.1$^+$Thy1.2$^+$), and KO B6 (Ametrine$^+$Thy1.1$^+$Thy1.2$^+$) T cells were mixed in equal numbers ($2.5\times10^6$ each; $10x10^6$ total cells)

and administered to mice with 6-day old hCD19$^+$ B-ALL tumors. For KO and DKO CAR-T cell co-transfers, activated CD8$^+$ CAR-Tg cells were transduced with Regnase-1-targeting sgRNA vector alone (mCherry) or with Regnase-1- targeting sgRNA (Ametrine) and Tcf7-targeting sgRNA (GFP) vectors together to generate KO (mCherry$^+$Thy1.1$^+$Thy1.2$^+$) and DKO (Ametrine$^+$GFP$^+$Thy1.1$^-$ Thy1.2$^+$) CAR-T cells. Transduced cells were sorted based on fluorescent reporter expression, mixed 5:1 ($2.5\times10^6$ KO and $0.5\times10^6$ DKO; $3\times10^6$ total cells) and administered to mice with 6-day old hCD19$^+$ B-ALL tumors. Spleens and bone marrow from tibia and femur were harvested at the indicated time points for flow cytometric analysis.

To evaluate recall response, activated CD8$^+$ WT and KO CAR-T cells were co-transferred to tumor-bearing mice as described above. WT and KO CAR-T cells were sorted from spleens 21 days later based on fluorescent reporter expression, mixed 1:1 ($1\times10^5$ each; $2\times10^5$ total cells) and transferred to naïve C57BL/6 recipients, followed by challenge with $1\times10^6$ hCD19$^+$ B-ALL cells the next day. Spleens were harvested 5 days later and transferred CAR-T cells were MACS-enriched using anti-CD8α MicroBeads (Miltenyi) prior to flow cytometric analysis.

*Flow cytometry*

Mouse cells were incubated in PBS containing 2% (wt/vol) BSA (Sigma) with flurochrome-conjugated anti-mouse antibodies against the following (antibody clones in parentheses): From Biolegend - CD69 (H1.2F3), CD44 (IM7), CD62L (MEL-14), CD127 (A7R34), CD8α (53-6.7), CD90.1/Thy1.1 (OX-7), CD90.2/Thy1.2 (30-H12), PD-1 (J43), TIGIT (1G9); From Thermo Fisher -

LAG3 (eBioC9B7W), KLRG1 (2F1). CAR surface expression on mouse CAR-Tg cells was detected with APC-labeled recombinant human CD19 (Creative Biomart; CD19-3309HA). Human cells were stained with fluorochrome-conjugated anti-human antibodies against the following: From Biolegend - CD45 (HI30), CD4 (OKT4), CD8α (HIT8a), CD45RA (HI100), CD45RO (UCHL1), CCR7 (G043H7), CD25 (BC96). CAR surface expression on human T cells was detected with recombinant human CD19Fc fusion protein (R&D Systems) followed by APC-conjugated goat anti-human IgG (Jackson Immunoresearch).

For intracellular cytokine staining, cells were stimulated in complete medium with Cell Stimulation Cocktail (Thermo Fisher) for 4–6 hours. Following surface staining, cells were fixed and permeabilized (Fixation/permeabilization kit; BD Biosciences). Mouse cells were stained with fluorochrome-conjugated anti-mouse antibodies against the following: From Biolegend - IFNγ (XMG1.2), TNFα (MP6-XT22), granzyme B (QA16A02); From Thermo Fisher - IL-2 (JES6-5H4). Human cells were stained with fluorochrome-conjugated anti-human antibodies against the following: From Biolegend - IFNγ (4S.B3), IL-2 (MQ1-17H12); From Thermo Fisher - TNFα (Mab11), granzyme B (GB11).

The Foxp3/Transcription Factor Staining Buffer Set (TONBO Biosciences) was used with fluorochrome-conjugated antibodies for intranuclear staining: From Thermo Fisher - Eomes (Dan11mag), Ki67 (SolA15); From Cell Signaling Technology - BATF (D7C5), TCF-1 (C63D9); From Miltenyi Biotech - TOX (REA473). 7-AAD (Sigma) was used for exclusion of dead cells in all

experiments. Samples were run on an LSRFortessa (BD) and data was analyzed using Flowjo v10 (Tree Star).

*Microarray differential expression analysis*

Expression signals were summarized by robust multiarray average algorithm Affymetrix Expression Console v1.1, followed by differential expression analysis performed using R package limma v.3.34.9. All plots were generated using R package ggplot2 v.2.2.1. Differentially expressed transcripts were identified by empirical Bayes test implemented in limma, and the Benjamini-Hochberg method was used to estimate the false discovery rate (FDR) as described.[3] Differentially expressed (DE) genes were defined by log2 FC > 0.5; adjusted $P < 0.05$.The remove Batch Effect function implemented in R package limma v.3.34.9 was used to correct batch effects.[4]

*Gene set enrichment analysis*

Gene Set Enrichment Analysis (GSEA) was performed using the C7 Immune Signatures database from MSigDB.[5,6] The microarray dataset (GSE84105) was used to generate the 'AHMED_CXCR5' gene set (< 5% FDR); RNA-seq data (GSE76279) were processed using DEseq2 R package v.1.16.1 to generate the 'YU_CXCR5' gene set as previously described.[3]

*Weighted gene correlation network analysis*

Weighted gene correlation network analysis (WGCNA) was performed using WGCNA R package v.1.66 as previously described.[4] Total mRNA co-expression clusters were defined using the top one third highly variable genes ranked by row variation followed by filtering the final clusters using DE criteria described above in at least one out of 4 comparisons. Pearson correlation matrix was calculated for each experiment followed by an adjacency matrix calculation by raising the correlation matrix to a power of 7 to meet the scale-free topology criterion. Co-expression clusters were defined by hybrid dynamic tree cutting method with minimum height for merging module set at 0.2. A consensus trend for each co-expression cluster was defined based on the first principal component, and cluster membership was defined as Pearson correlation between individual genes and the consensus trend of the co-expression cluster. Genes were assigned to the most correlated co-expression cluster with cutoff of $r \geq 0.7$. This resulted in 1856 genes in ten distinct gene clusters (Clusters 1-10) and an additional 201 genes that met significance thresholds but could not be clustered (Cluster 0).

*Bisulfite sequencing methylation profiling and data analysis*

Co-transfer of $CD8^+$ WT and KO CAR-T cells into tumor-bearing mice were performed as described above and transferred cells were isolated from spleens 21 days later by FACS based on fluorescent reporter and congenic marker expression. Genomic DNA was isolated and a bisulfite-modified DNA-sequencing library was generated as previously described.[7] Sequencing data were aligned to the mm10 genome using BSMAP2.74.[8] Differentially methylated regions (DMRs) were identified using Bioconductor package DSS.[9] Statistical test of differentially methylated locus (DML) was performed using DMLtest function (smoothing = TRUE) in DSS followed by detection

of differentially methylated regions using CallDMR function in DSS. The thresholds for defining a DMR were a p value <0.01, minimum length of 50 bps, and minimum of 3 CpG sites.

*Generation of human Regnase-1 KO CD19 CAR-T cells*

A 1,538bp EcoRI-XhoI fragment from the retroviral vector, MSCV-antiCD19BBz[10], consisting of the anti-CD19 CAR open reading frame was cloned into a third-generation lentiviral vector under the control of the MND promoter to make pCL45-MND-CD19CAR. Lentiviral supernatant was produced and titrated as previously described.[11] Bulk $CD4^+$ and $CD8^+$ T cells were isolated from human PBMCs using the Pan T cell isolation kit (Miltenyi), activated with 2 μg/ml anti-human CD3/CD28 overnight, and transduced with viral supernatant at 1150 x g for 15 minutes to generate human CD19 CAR-T cells.

For deletion of Regnase-1 in human CD19 CAR-T cells, working stocks of 100 μM Regnase-1-targeting or control non-targeting sgRNAs and 40 μM purified Cas9-NLS protein (University of California, Berkeley) were prepared. The ribonucleoprotein (RNP) complex was prepared by mixing 180 pmol of sgRNA and 40 pmol of Cas9 protein (total volume of 2.8 μl). CD19 CAR-T cells ($5x10^5$) were resuspended in 20 μl of Lonza P3 buffer (Lonza AmaxaTM P3 primary cell 96-well NucleofectorTM Kit; Cat. No. V4SP-3096), mixed with the RNP complex, and electroporated. Pre-warmed complete RPMI media (80 μl) was added to each cuvette and cells were rested for 15 mins at 37°C. Cells were cultured in 24 well plates in complete RPMI medium with 5 ng/ml IL-7 and IL-15 for 4-7 days prior to functional analysis.

Three sgRNAs targeting human Regnase-1 were assessed individually in human CD19 CAR-T cells for editing efficiency. Regnase-1 KO CAR-T cells generated with either sgRNA-1 or sgRNA-3 yielded comparable results in *in vitro* functional studies. Representative data from Regnase-1 KO CAR-T cells generated with sgRNA-1 is shown in all figures.

*Targeted amplicon library preparation, sequencing, and analysis*

Targeted amplicons were generated using gene-specific primers with partial Illumina adapter overhangs (RL122.F – 5'-GACCACCCAACCCCGTTTCCTGTGC-3' and RL122.R – 5'-CCAGGCTGCACTGCTCACTCTCTGT-3' or RL120.F-TCTTGCCCCGGTGACCTTGGCGTTA-3' and RL120.R – 5'-TGTGGACCCCAAGTCTGTCAGGGCC-3', overhangs not shown) and sequenced as previously described.[12] Briefly, cell pellets were lysed and used to generate gene-specific amplicons with partial Illumina adapters in PCR#1. Amplicons were indexed in PCR#2 and pooled with other targeted amplicons for other loci to create sequence diversity. Additionally, 10% PhiX Sequencing Control V3 (Illumina) was added to the pooled amplicon library prior to running the sample on an Miseq Sequencer System (Illumina) to generate paired 2 x 250bp reads. Samples were demultiplexed using the index sequences, fastq files were generated, and NGS analysis was performed using CRIS.py.[13]

*Immunoblotting*

Human CD19 CAR-T cells targeted with control sgRNA or Regnase-1-targeting sgRNA were resuspended in lysis buffer (150 mM NaCl, 50 mM Tris pH 8, 1% NP-10, and 0.25% sodium deoxycholate with added phosphatase and protease inhibitors). Lysates were run on a 4-12% Bis-Tris Gel (Invitrogen), and transferred to PVF. Membranes were blocked with 5% milk and incubated with anti-human/mouse Regnase-1 (R&D systems, MAB7875) followed by HRP-anti mouse IgG. Pierce ECL substrate was added to membranes and signal was detected with ChemiDoc Touch Imaging System (BIO-RAD).

*sgRNA sequences*

The following sgRNAs were used in murine CAR-Tg cells: non-targeting control: 5'-ATGACACTTACGGTACTCGT-3'; *Regnase-1*: 5'-AAGGCAGTGGTTTCTTACGA-3' and 5'-GGAGTGGAAACGCTTCATCG-3'; *Tcf7*: 5'-CTTCGGTCACTTACCAGCGG-3'. The following sgRNAs were used in human CAR-T cells: non-targeting control: 5'-GCUUGUGGAUGUUGCGGAAGNGG-3'; human *Regnase-1*: sgRNA-1: 5'-TTCACACCATCACGACGCGTNGG-3'; sgRNA-2: 5'-TGGGGGCAGCTTGGCCGCTCNGG-3'; sgRNA-3: 5'-CAGCTCCCTCTAGTCCCGCGNGG-3'.

**Supplemental Figure 1**

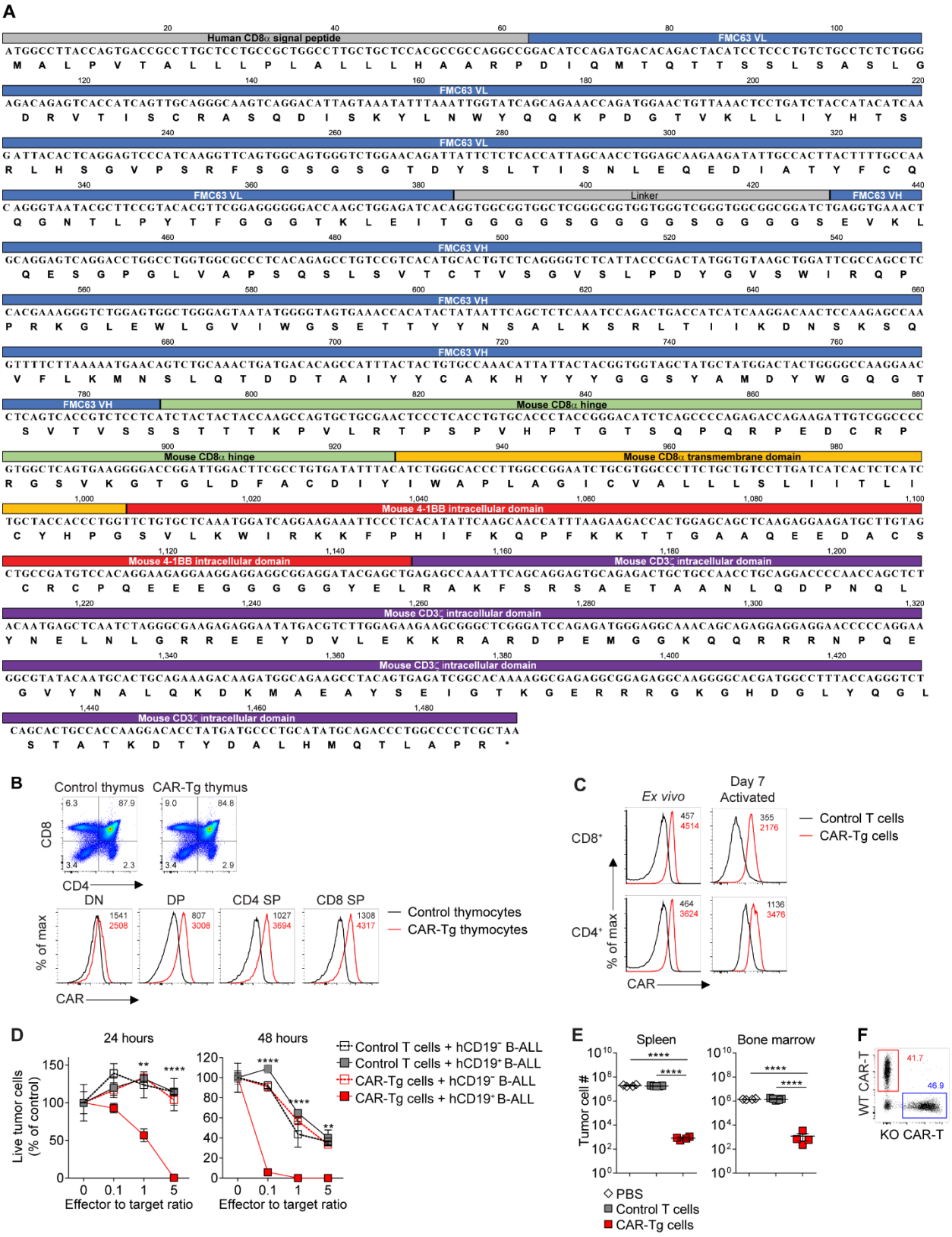

**Supplemental Figure 1. Targeting Regnase-1 unleashes durable CAR-T cell-mediated protection in an immune competent leukemia model.** (A) cDNA sequence of CD19 CAR construct used to generate CAR-Tg mice. (B) Frequencies of thymic populations (top) and mean fluorescence intensities (MFI) of CAR surface expression (bottom) in control and hCD19 CAR-Tg thymocytes assessed by flow cytometry. (C) CAR expression and MFI of splenic $CD4^+$ and $CD8^+$ T cells from control or CAR-Tg mice assessed by flow cytometry directly *ex vivo* (left), or 7 days after activation (right). (D) Activated control or CAR-Tg cells were co-cultured with $hCD19^-$ or $hCD19^+$ B-ALL cells for 24 or 48 hours. Live tumor cells were enumerated by quantitative flow cytometry and normalized to control cultures without T cells. (E) Mice bearing $hCD19^+$ B-ALL tumors were treated with PBS or activated control or CAR-Tg cells (1:1 $CD4^+$:$CD8^+$). Spleen and bone marrow were harvested 7 days later for flow cytometric analysis. Number of $hCD19^+$ B-ALL tumor cells. (F) $CD8^+$ WT and KO CAR-T cells were co-transferred 1:1 into tumor-bearing mice. Representative pre-transfer populations of WT and KO CAR-T cells. Data are shown as mean ± SEM and representative of 2 (B, D; n=2 mice/group) or 3 (C, E-F; n=5 mice/group) independent experiments. Significance was determined by two-way ANOVA with Tukey's post-test for multiple comparisons (D) or one-way ANOVA with Tukey's post-test for multiple comparisons (E). $*P < .05$; $**P < .01$; $***P < .001$; $****P < .0001$.

**Supplemental Figure 2**

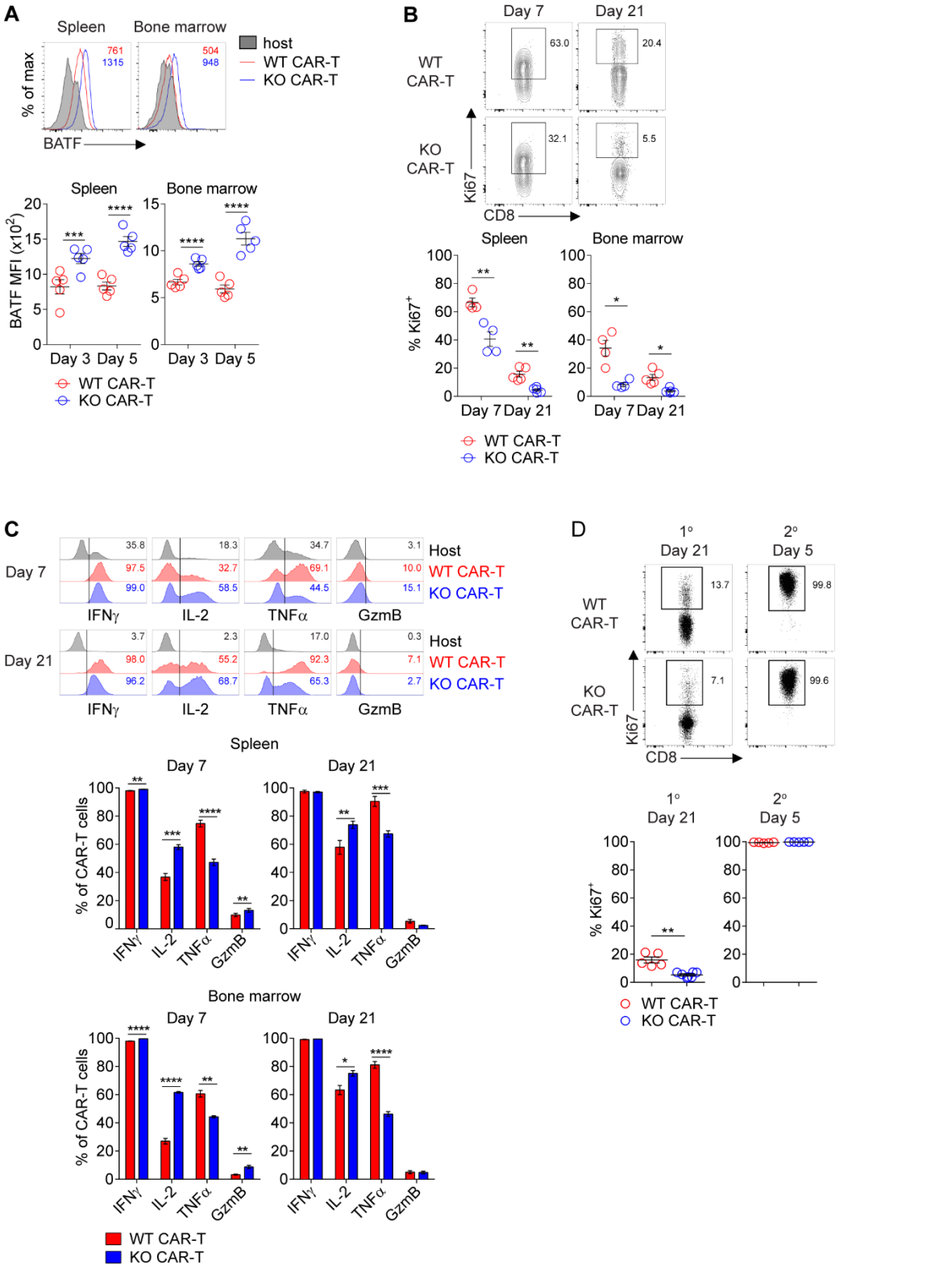

**Supplemental Figure 2. Regnase-1 deletion promotes formation of memory-like CAR-T cells capable of recall responses.** (A-C) $CD8^+$ WT and KO CAR-T cells were co-transferred 1:1 into tumor-bearing mice. Organs were harvested at the indicated time points for analysis. (A) Representative histograms (day 5 only) and BATF MFI in WT and KO CAR-T cells. (B) Representative dot plots (spleen only) and frequency of $Ki67^+$ WT and KO CAR-T cells. (C) Representative histograms and frequencies of $IFN\gamma^+$, $IL\text{-}2^+$, $TNF\alpha^+$ and granzyme $B^+$ (GzmB) WT and KO CAR-T cells. Endogenous host $CD8^+$ T cells are shown as a gating control. (D) $CD8^+$ WT and KO CAR-T cells were co-transferred 1:1 into tumor-bearing mice, sorted from spleens 21 days later, and co-transferred 1:1 again into naïve recipients that received $hCD19^+$ B-ALL cells the following day. Spleens were harvested 5 days later for analysis. Frequencies of $Ki67^+$ WT and KO CAR-T cells 21 days after primary tumor stimulation (left) and 5 days after secondary co-transfer and tumor stimulation (right) are shown. Data are shown as means ± SEM and representative of 2 (D) or 3 (A-C) independent experiments (n=3-5 mice per group) Significance was determined by paired *t* test (A-D). $*P < .05$; $**P < 0.01$; $***P < .001$; $****P < .0001$.

**Supplemental Figure 3**

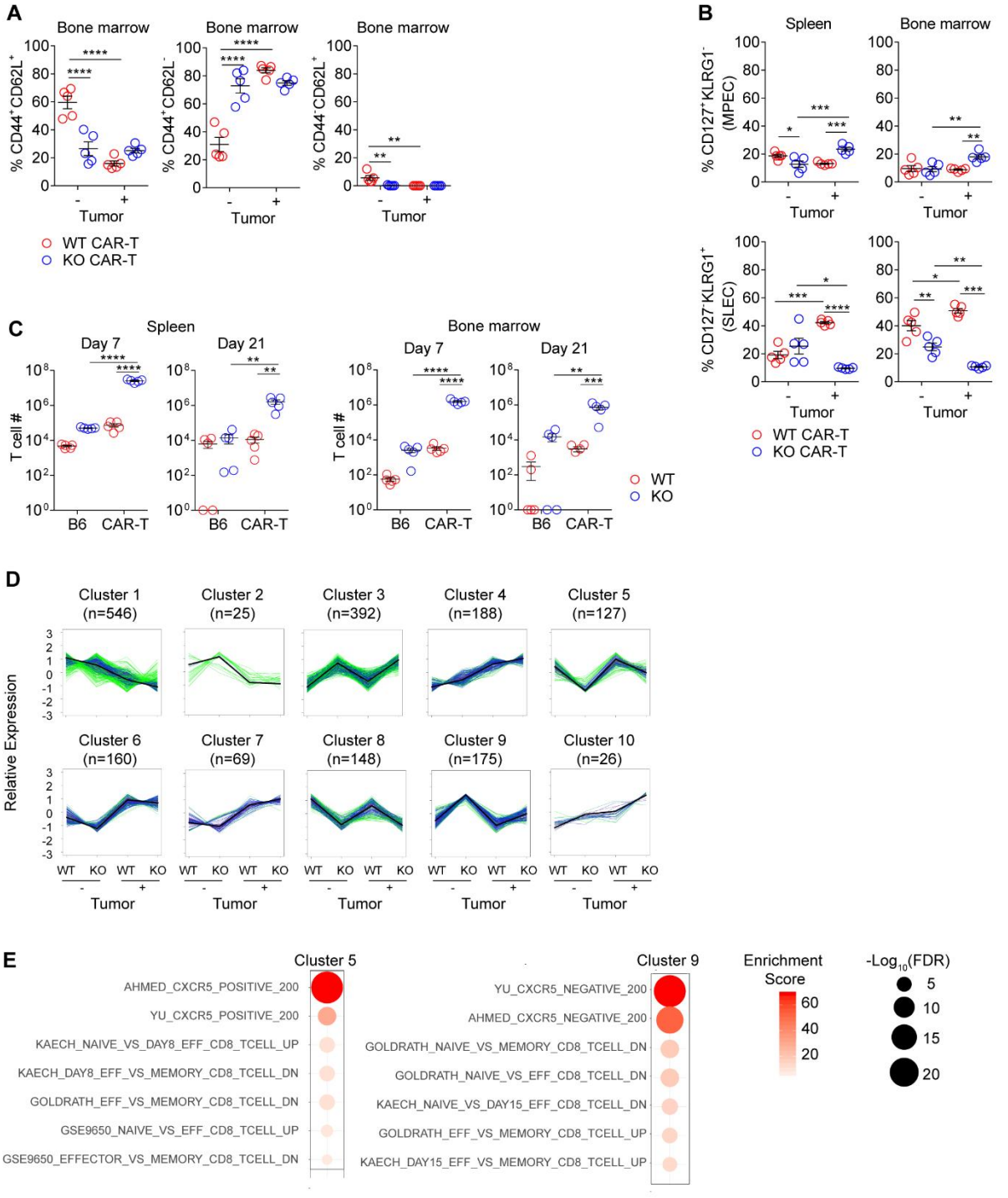

**Supplemental Figure 3. Regnase-1 KO CAR-T cells undergo tumor-dependent reprogramming from effector to memory-like cells.** $CD8^+$ WT and KO CAR-T cells were co-transferred 1:1 into mice with or without tumors. Organs were harvested 7 days after co-transfer for flow cytometric or microarray analysis. (A) Frequencies of $CD44^+CD62L^-$, $CD44^+CD62L^+$ and $CD44^+CD62L^-$ WT and KO CAR-T cells. (B) Frequencies of $CD127^+KLRG1^-$ and $CD127^-KLRG1^+$ WT and KO CAR-T cells. (C). $CD8^+$ WT CAR-T, KO CAR-T, WT B6, and KO B6 T cells were mixed in equal numbers ($2.5\times10^6$ each, $10x10^6$ total cells) and administered to mice with 6-day old $hCD19^+$ B-ALL tumors. Number of cells in the spleen and bone marrow 7 and 21 days after transfer is shown. (D-E) Microarray analysis of transcripts from $CD8^+$ WT and KO CAR-T cells. Weighted Gene Correlation Network Analysis (WGCNA) was performed on the top third of variable genes across 4 pair-wise comparisons: KO versus WT without tumor, KO versus WT with tumor, KO with versus without tumor, and WT with versus without tumor; followed by filtering for DE genes at FDR < 0.05 and $\log_2FC > 0.5$ in at least one comparison. (D) Relative expression plots of WGCNA gene clusters. (E) Gene set enrichment analysis (GSEA) plots of gene clusters 5 and 9 (identified by WCGNA) compared to the C7 Immune Signatures database from MSigDB and manually curated gene signatures from public datasets. Functional enrichment analysis was performed using fisher's exact test. Significant pathways were selected at BH adjusted $P < 0.05$. Data are shown as mean ± SEM and represent 3 independent experiments (A-C; n=4-5 mice/group). Microarrays were run with n=3-5 mice/group (D-E). Significance was determined by two-way ANOVA with Tukey's post-test for multiple comparisons (A-C). *$P < .05$; **$P < .01$; ***$P < .001$; ****$P < .0001$.

**Supplemental Figure 4**

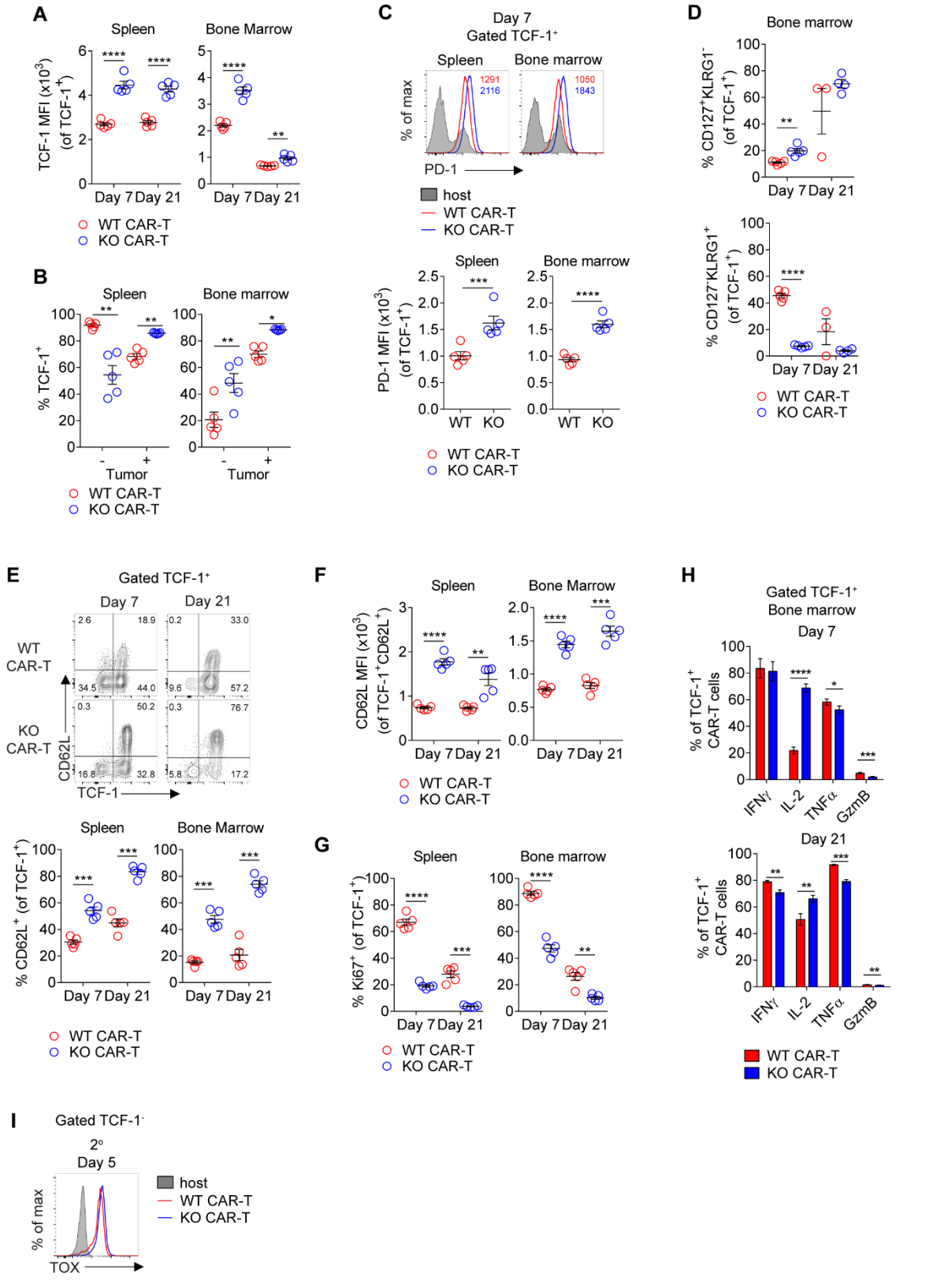

**Supplemental Figure 4. Regnase-1 limits formation of TCF-1$^+$ precursor exhausted CAR-T cells and reduces their memory phenotype.** CD8$^+$ WT and KO CAR-T cells were co-transferred 1:1 into tumor-bearing or tumor-free mice. Organs were harvested at the indicated time points. (A) Mean fluorescent intensity (MFI) of TCF-1 in TCF-1$^+$ WT and KO CAR-T cells from tumor-bearing mice. (B) Frequency of TCF-1$^+$ WT and KO CAR-T cells in tumor-bearing or tumor-free mice 7 days after co-transfer. (C) Representative histograms and MFI of PD-1 on TCF-1$^+$ WT and KO CAR-T cells from tumor-bearing mice. (D) Frequencies of TCF-1$^+$CD127$^+$KLRG1$^-$ and TCF-1$^+$CD127$^-$KLRG1$^+$ WT and KO CAR-T cells in the bone marrow of tumor-bearing mice. (E) Representative plots and frequencies of TCF-1$^+$CD62L$^+$ WT and KO CAR-T cells from spleens of tumor-bearing mice. (F) MFI of CD62L on TCF-1$^+$CD62L$^+$ WT and KO CAR-T cells from tumor-bearing mice. (G) Frequencies of TCF-1$^+$Ki67$^+$ WT and KO CAR-T cells from tumor-bearing mice. (H) Frequencies of TCF-1$^+$IFNγ$^+$, TCF-1$^+$IL-2$^+$, TCF-1$^+$TNFα$^+$ and TCF-1$^+$granzyme B$^+$ (GzmB) WT and KO CAR-T cells in the bone marrow of tumor-bearing mice. (I) CD8$^+$ WT and KO CAR-T cells were co-transferred 1:1 into tumor bearing mice and sorted from spleens 21 days later. Sorted cells (> 90% TCF-1$^+$) were co-transferred 1:1 into naïve recipients that received hCD19$^+$ B-ALL cells the following day. Spleens were harvested 5 days later. Representative histogram showing TOX expression on TCF-1$^-$ WT and KO CAR-T cells 5 days after secondary co-transfer and tumor stimulation is shown. Data are shown as mean ± SEM (A-H) and are representative of 2 (I) or 3 (A-H) independent experiments with 3-5 mice/group Significance was determined by paired *t* test. **P* < .05; ***P* < .01; ****P* < .001; **** < .0001.

**Supplemental Figure 5**

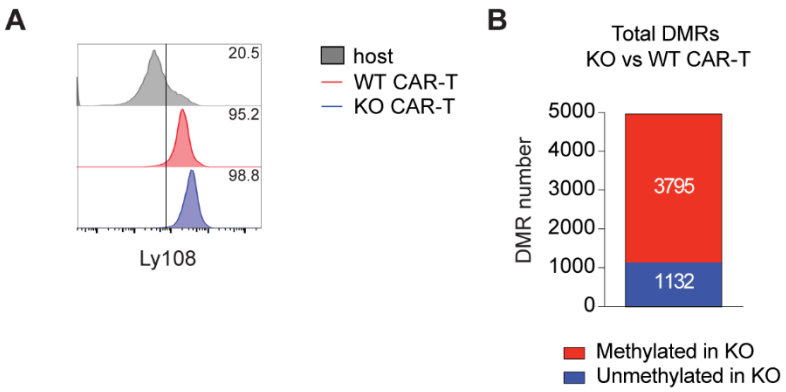


**Supplemental Figure 5. Regnase-1 KO CAR-T cells acquire memory, effector, and exhaustion associated epigenetic programs.** $CD8^+$ WT and KO CAR-T cells were co-transferred 1:1 into tumor-bearing mice and $CD8^+Ly108^+$ cells were sorted from spleens 21 days later for whole-genome DNA methylation profiling. (A) Representative histograms showing Ly108 expression on sorted $CD8^+$ WT and KO CAR-T cells. Endogenous host $CD8^+$ T cells are shown as control. (B) Proportion of methylated versus unmethylated differentially methylated regions (DMRs) in KO compared with WT CAR-T cells. Data represent 10 biological replicates pooled into 3 samples for analysis in triplicate.

**Supplemental Figure 6**

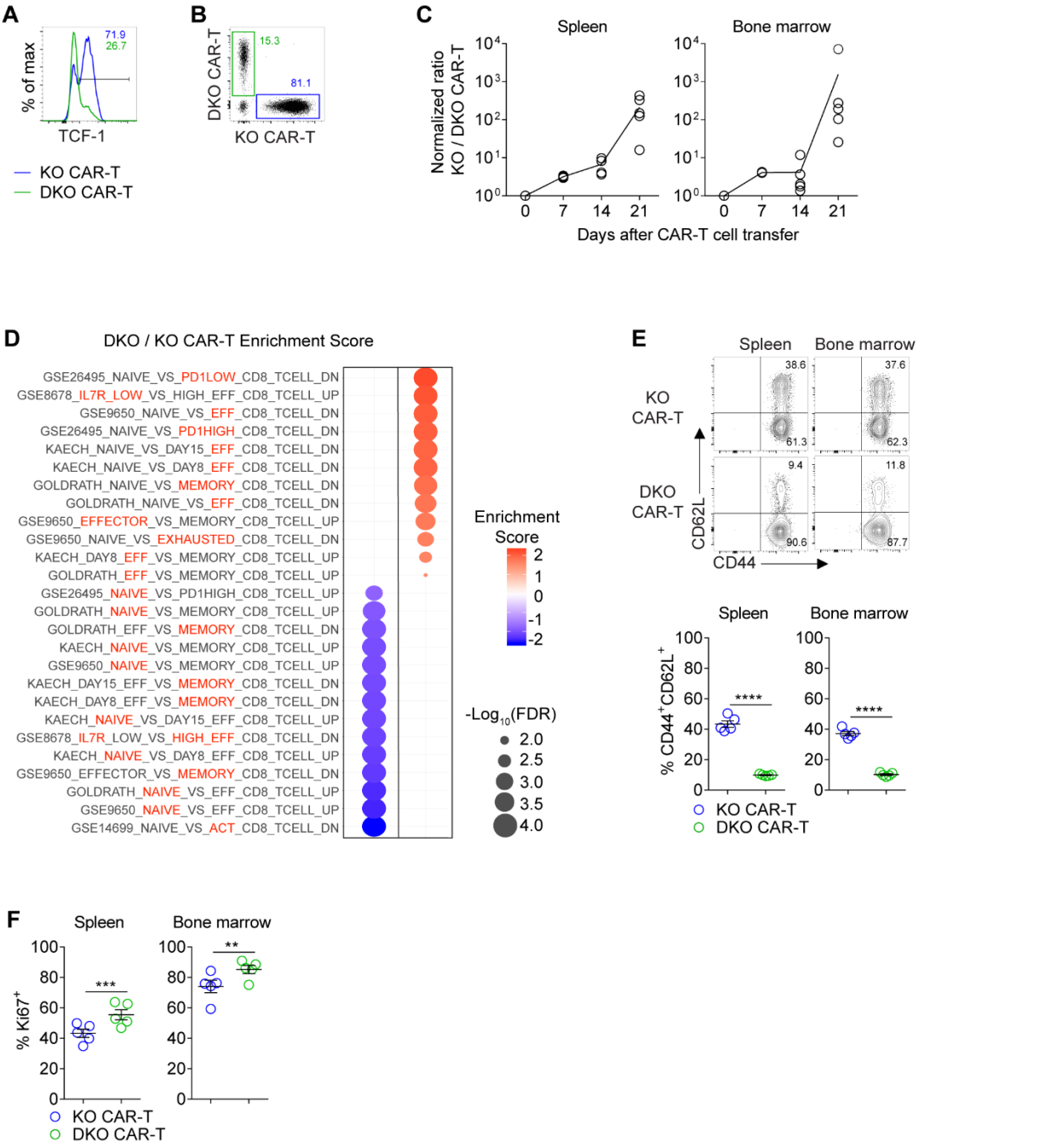

**Supplemental Figure 6. Improved persistence and expanded $T_{PEX}$ formation in Regnase-1 KO CAR-T cells is TCF-1-dependent.** Naïve MACS-purified $CD8^+Cas9^+$ hCD19 CAR-Tg cells were activated and transduced with sgRNA targeting Regnase-1 (KO CAR) or Regnase-1 and *Tcf7* (DKO CAR). Cells were sorted based on fluorescent reporter expression and co-transferred 5:1 (KO:DKO) into tumor-bearing mice. Organs were harvested at the indicated time points. (A) Representative frequencies of TCF-$1^+$ cells in KO and DKO CAR-T cells before co-transfer. (B) Representative pre-transfer frequencies of KO and DKO CAR-T cells in co-transfer experiment. (C) Cell numbers normalized to pre-transfer ratio and plotted as normalized ratio of KO to DKO CAR-T cells. (D) GSEA plots of microarray data from DKO and KO CAR-T cells from the spleens of tumor-bearing mice 7 days after co-transfer. The ratio of gene expression between DKO and KO CAR-T cells was compared to the C7 Immunologic signatures gene set collection (DN=downregulated; UP=upregulated). Red circles represent enrichment in DKO CAR-T while blue circles represent enrichment in KO CAR-T. The enriched subset in each gene set is highlighted in red. (E) Representative plots and frequencies of $CD44^+CD62L^+$ KO and DKO CAR-T cells from tumor-bearing mice 7 days after co-transfer. (F) Frequencies of $Ki67^+$ KO and DKO CAR-T cells from tumor-bearing mice 7 days after co-transfer. Data are shown as mean ± SEM (E-F) and representative of 2 independent experiments (A-C, E-F; n=5 mice/group). Microarrays were run with n=3-5 mice/group. Significance was determined by paired *t* test (E-F). **P* < .05; ***P* < .01; ****P* < .001; *****P* < .0001.

**Supplemental Figure 7**

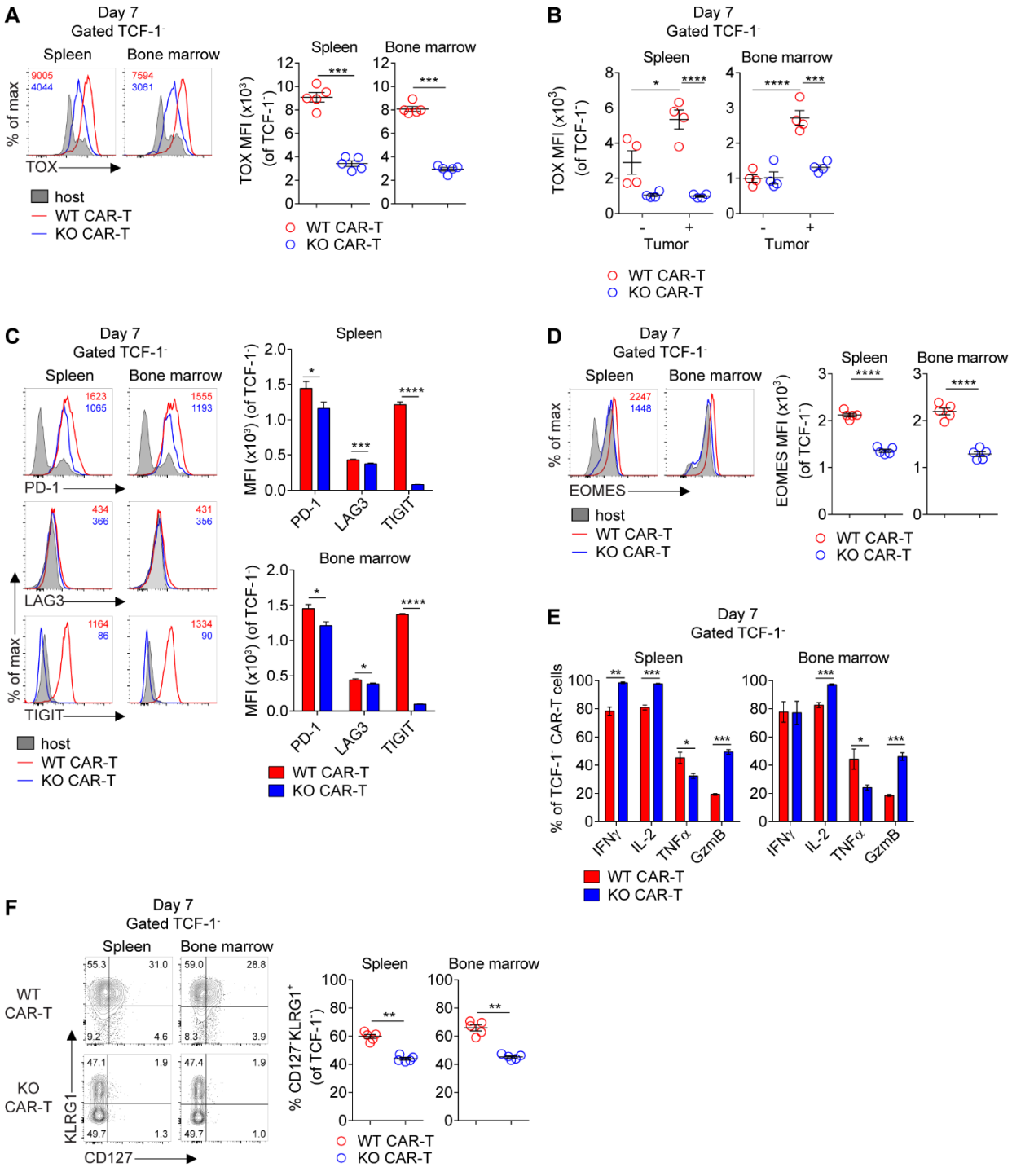

**Supplemental Figure 7. Regnase-1 promotes exhaustion of TCF-1$^{-}$ CAR-T cells.** CD8$^{+}$ WT and KO CAR-T cells were co-transferred 1:1 into tumor-bearing or tumor-free mice. Organs were harvested 7 days later. (A) TOX MFI in TCF-1$^{-}$ WT and KO CAR-T cells. (B) MFI of TOX in TCF-1$^{-}$ WT and KO CAR-T cells. (C) MFI of PD-1, LAG3, and TIGIT in TCF-1$^{-}$ WT and KO CAR-T cells. (D) MFI of EOMES in TCF-1$^{-}$ WT and KO CAR-T cells. (E) Frequencies of TCF-1$^{-}$IFNγ$^{+}$, TCF-1$^{-}$IL-2$^{+}$, TCF-1$^{-}$TNFα$^{+}$ or TCF-1$^{-}$granzyme B$^{+}$ WT and KO CAR-T cells. (F) Frequencies of TCF-1$^{-}$CD127$^{-}$KLRG1$^{+}$ WT and KO CAR-T cells. Data are shown as mean ± SEM and representative of 3 independent experiments (A-F; n=4-5 mice/group). Significance was determined by paired *t* test (A-F). **P* < .05; ***P* < .01; ****P* < .001; *****P* < .0001.

**Supplemental References**


1. Nicholson IC, Lenton KA, Little DJ, et al. Construction and characterisation of a functional CD19 specific single chain Fv fragment for immunotherapy of B lineage leukaemia and lymphoma. *Mol Immunol*. 1997;34(16-17):1157-1165.

2. Greaves DR, Wilson FD, Lang G, Kioussis D. Human CD2 3'-flanking sequences confer high-level, T cell-specific, position-independent gene expression in transgenic mice. *Cell*. 1989;56(6):979-986.

3. Wei J, Long L, Zheng W, et al. Targeting REGNASE-1 programs long-lived effector T cells for cancer therapy. *Nature*. 2019;576(7787):471-476.

4. Tan H, Yang K, Li Y, et al. Integrative Proteomics and Phosphoproteomics Profiling Reveals Dynamic Signaling Networks and Bioenergetics Pathways Underlying T Cell Activation. *Immunity*. 2017;46(3):488-503.

5. Godec J, Tan Y, Liberzon A, et al. Compendium of Immune Signatures Identifies Conserved and Species-Specific Biology in Response to Inflammation. *Immunity*. 2016;44(1):194-206.

6. Miller BC, Sen DR, Al Abosy R, et al. Subsets of exhausted CD8(+) T cells differentially mediate tumor control and respond to checkpoint blockade. *Nat Immunol*. 2019;20(3):326-336.

7. Abdelsamed HA, Moustaki A, Fan Y, et al. Human memory CD8 T cell effector potential is epigenetically preserved during in vivo homeostasis. *J Exp Med*. 2017;214(6):1593-1606.

8. Xi Y, Li W. BSMAP: whole genome bisulfite sequence MAPping program. *BMC Bioinformatics*. 2009;10:232.

9. Wu H, Xu T, Feng H, et al. Detection of differentially methylated regions from whole-genome bisulfite sequencing data without replicates. *Nucleic Acids Res*. 2015;43(21):e141.

10. Imai C, Mihara K, Andreansky M, et al. Chimeric receptors with 4-1BB signaling capacity provoke potent cytotoxicity against acute lymphoblastic leukemia. *Leukemia*. 2004;18(4):676-684.

11. Bauler M, Roberts JK, Wu CC, et al. Production of Lentiviral Vectors Using Suspension Cells Grown in Serum-free Media. *Mol Ther Methods Clin Dev*. 2020;17:58-68.

12. Sentmanat MF, Peters ST, Florian CP, Connelly JP, Pruett-Miller SM. A Survey of Validation Strategies for CRISPR-Cas9 Editing. *Sci Rep*. 2018;8(1):888.

13. Connelly JP, Pruett-Miller SM. CRIS.py: A Versatile and High-throughput Analysis Program for CRISPR-based Genome Editing. *Sci Rep*. 2019;9(1):4194.